Available online at www.sciencedirect.com

ScienceDirect

Procedia Structural Integrity 38 (2022) 581–587

Structural Integrity Procedia

www.elsevier.com/locate/procedia

FATIGUE DESIGN 2021, 9th Edition of the International Conference on Fatigue Design

High Temperature Tensile and Fatigue Behaviors of Additively Manufactured IN625 and IN718

Reza Ghiaasiaan[a,b], Arun Poudel[a,b], Nabeel Ahmad[a,b], Paul R. Gradl[c], Shuai Shao[a,b], Nima Shamsaei[a,b*]

[a]*Department of Mechanical Engineering, Auburn University, Auburn, AL 36849, USA*
[b]*National Center for Additive Manufacturing Excellence (NCAME), Auburn University, Auburn, AL 36849, USA*
[c]*NASA Marshall Space Flight Center, Propulsion Department, Huntsville, AL 35812, USA*

Abstract

Recent advancement and research efforts in additive manufacturing (AM) have made it a promising technology to fabricate nickel-base superalloy parts in near net shapes. IN625 and IN718 are the commonly used superalloys in elevated-temperature applications in the aerospace and energy sectors. However, the fatigue performance of the additively manufactured (AM) components often depends on the defects like porosity, micro-cracks, and lack-of-fusions, etc. In addition, the presence of columnar grains and residual stresses also affects their fatigue performance. In this study, IN625 and IN718 specimens were fabricated via both laser powder bed fusion (L-PBF) and laser powder directed energy deposition (LP-DED) followed by stress-relief and standard heat treatments. Both alloys exhibited similar defect characteristics and grain morphologies. High-temperature fatigue properties of both IN625 and IN718 were tested at two strain amplitudes of 0.005 and 0.01 mm/mm and at two elevated temperatures of 427 and 625 °C. The fatigue lives of both alloys decreased with increasing testing temperatures. AM IN718 showed inferior fatigue performance at both test temperature and strain amplitudes in L-PBF conditions while in LP-DED condition both alloys have shown comparable fatigue performance.

Keywords: Laser powder bed fusion (L-PBF); Laser powder direct energy deposition (LP-DED) Ni-base superalloys; Fatigue

* Corresponding author. Tel.: +1-334-844-4839; fax: +1-334-844-3307.
E-mail address: shamsaei@auburn.edu

10.1016/j.prostr.2022.03.059

1. Introduction

Nickel-base superalloys are primarily used in components of jet engines and land-based turbines where the cyclic load capacity and fatigue response of the components are critically important properties (Donachie and Donachie, 2002). Despite their complex chemistry, the microstructure of Ni-base superalloys seems to be relatively simple. It can be either purely solid solution strengthened or consist of relatively small (50–1000 nm diameter) strengthening particles, such as ɣ' and ɣ" precipices (with $Ni_3(Al,Ti)$ $L1_2$ and Ni_3Nb $D0_{22}$ lattice structures, respectively), coherently/semi-coherently embedded in an FCC solid solution matrix, resulting in good elevated-temperature mechanical properties (Antolovich, Rosa and Pineau, 1981). The grain structure of Ni-base superalloys vary depending on the processing methods, ranging from dendritic with primary arm diameter as small as a few μm in the additively manufactured (AM) (Ghiaasiaan *et al.*, 2021) to fine grains in powder metallurgy alloys, and to single crystals as large as the actual size of the component such as the turbine blades (Donachie and Donachie, 2002). The fatigue behavior of the Ni-base superalloy can highly depend upon the defect-/micro- structure (Antolovich and Armstrong, 2014), deformation mode, and environment (Nezhadfar, Johnson and Shamsaei, 2020). Particularly, the typical AM process induced defects such as surface roughness and volumetric defects can severely limit the fatigue resistance of AM parts. Variations in alloy composition as well AM process parameters may alter the microstructure and defect content in AM Ni-base superalloys and consequently alter the cyclic response particularly at elevated temperatures (Antolovich and Armstrong, 2014).

In this paper, we have studied the strain-controlled fatigue responses of the AM IN 625 and IN 718 manufactured by laser powder bed diffusion (L-BPF) and laser powder direct energy deposition (LP-DED) processes. The fatigue lives of the alloys were measured and compared at two different strain levels (i.e., ε_a = 0.01 and 0.005 mm/mm) and at two elevated temperatures, i.e., 427 and 649 °C.

2. Experimental Procedure

The process parameters used for fabrication of the LP-DED and L-PBF test specimens in this study are listed in Table 1. The LP-DED and L-PBF test specimens were fabricated by the RPM Innovations (Rapid City, SD) and Carpenter Additive (Philadelphia, PA), respectively. Further, the chemical compositions of the powders used in this study is listed in Table 2, which is further shown by comparative bar charts in Fig. 1. It is notable that the chemical compositions were measured by Inductively Coupled Plasma (ICP) spectroscopy and reported by the manufacturer. The test specimens were heat treated prior to testing according to the procedures listed in Table 3 which are schematically illustrated in Fig. 2. The test specimens were heat treated in a vacuum furnace using an external thermocouple attached to the specimens to maintain the temperature deviation during the heat treatment within ±5 °C from the set temperature. The heat treatment procedures was performed according to the ASTM F3055-14a (ASTM International, 2014a) for AM IN 718 and the ASTM F3056-14a (ASTM International, 2014b). for AM IN 625.

Table 1. AM process parameters used for fabrication of Ni-base superalloy test specimens used in this study.

Process	Power (W)	Layer height (μm)	Travel speed (mm/min)
LP-DED	1070	381	1016
L-PBF	180-200	30-40	60,000

The microstructure of test specimens in fully heat-treated conditions was characterized in the normal direction (ND) plane, i.e., the plane perpendicular to the build direction. Metallography procedure were performed according to ASTM-E3 (ASTM International, 2012). For microstructural characterization, a Zeiss Crossbeam 550 scanning electron microscope (SEM) equipped with energy dispersive spectroscopy (EDS) and electron backscatter diffraction (EBSD) detectors was used. Backscattered secondary electron (BSE) micrographs were obtained using the electron channeling contrast imaging (ECCI) technique (Zaefferer and Elhami, 2014).

The fatigue tests were performed under uniaxial, fully-reversed ($R_\varepsilon = \varepsilon_{min}/\varepsilon_{max} = -1$), and strain-controlled condition at elevated temperatures of 427 and 649 °C for two strain amplitudes of 0.005 and 0.01 mm/mm according to the ASTM E606 standard (ASTM International, 2019). Tests were considered concluded upon final fracture or exceeding 10^7 reversals (i.e., as runouts).

Table 2. Chemical compositions in wt.% of the Ni-base superalloy powders used for fabrication of the AM specimens used in this study.

Powder	Ni	Cr	Mo	Co	Fe	Nb+Ta	Ti+Al	Powder Manufacturer
IN 718	52.5	19	3.1	1	16.8	5	1.5	AP&C (a GE additive company)
IN 625	63	21.5	9	1	5	3.7	0.8	Visser Precision

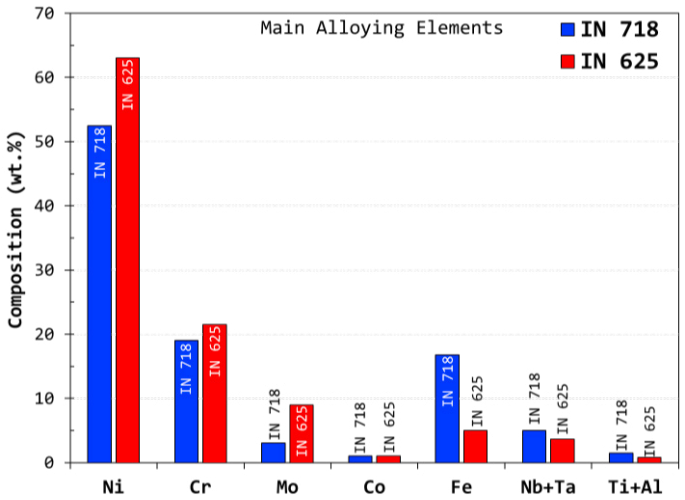

Fig. 1. Comparative bar chart of the main alloying elements for IN 718 and IN 625 powders used in this study. Note the chemical compositions were reported by the manufacturers of the powders.

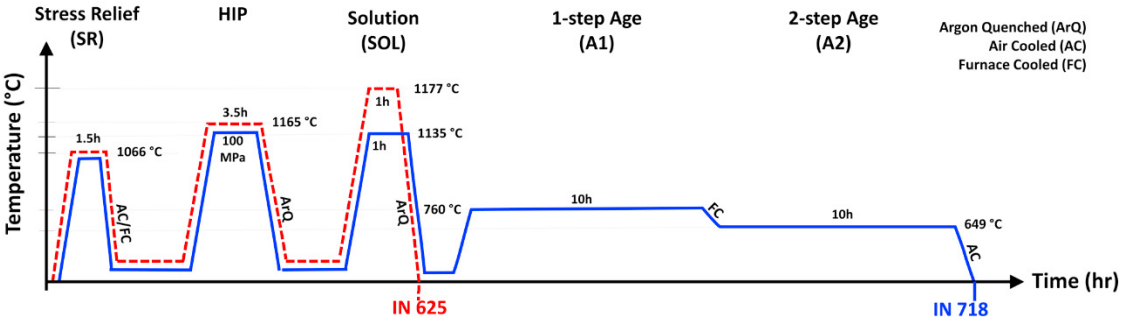

Fig. 2. Schematic diagram for the heat treatment schedules used for the AM IN 625 and IN 718 alloys investigated in this study.

Further, a Zeiss Xradia 620 Versa X-ray Computed Tomography (XCT) machine was used for the determination of defect content of the test specimens. The XCT scan results have been obained from the gauge section of the test specimens using a source voltage and power of 160 kV and 25 W, respectively. A total of 4000 projections were taken with the exposure time of each projection being 2s. A photon transmittance >5% and photon intensity of >5000 counts per pixel was achieved at the mid section of the gage. The volxel size of the scan was ~6 μm.

Table 3. List of heat treatment processes used in this study for the AM IN 625 and IN 718 alloys.

Materials	Stress Reliving (SR)	Hot Isostatic Pressing (HIP)	Solutionizing (SOL)	Ageing	
				1-step (A1)	2-step (A2)
	Temperature-°C/Holding Time-hr/(Pressure-MPa)/Quench Medium				
IN 718	1066°C /1.5h/Argon	1165°C /3.5h/100MPa/Air	1165°C /1h/Argon	760°C /10h/Furnace	649°C /10h/Air
IN 625			1177°C /1h/Argon	NA	

3. Results and Discussion

Inverse pole figure (IPF) maps for the non-heat treated (NHT) and heat-treated LP-DED IN 625 and IN 718 alloys are presented in Fig. 3. The average grain sizes are also reported on the IPF maps shown in Fig. 3. It should be noted that the grain sizes are slightly increased after heat treatments for both IN 625 LP-DED and IN 718 LP-DED alloys. The typical BSE SEM micrographs for the non-heat treated (NHT) and fully heat-treated conditions of all the AM IN 625 and IN 718 alloys are presented in Fig. 4. As shown, the prior inter-dendritic regions observed in NHT condition are removed after the full heat treatment processes for both the IN 625 LP-DED as well as the IN 718 LP-DED alloys. As shown in high magnification BSE micrographs for the IN 718 alloys, the plate-like ɣ”-precipitates are discernable (see Fig. 4 (c)). Furthermore, Fig. 5 presents the typical XCT scan results obtained from the gauge sections of IN 718 LP-DED and IN 625 LP-DED test specimens in both NHT and post-hot isostatic pressing (HIP) conditions. As shown, upon HIP, the amount of AM induced defects such as pores are significantly reduced (Shao *et al.*, 2017).

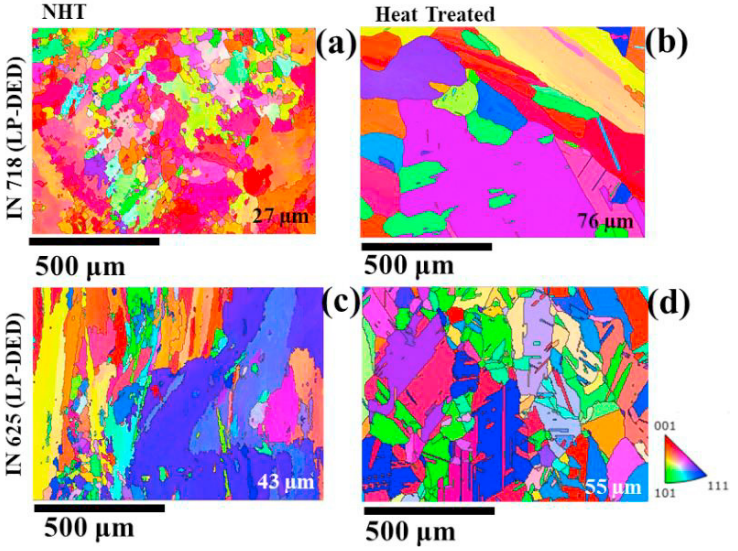

Fig. 3. Inverse pole figure (IPF) maps obtained in the ND plane (the plane perpendicular to building direction) for some Ni-base superalloys investigated in this study in non-heat treated (NHT) and fully heat treated conditions as listed in Table 3: (a)-(b) LP-DED IN 718 and (c)-(d) LP-DED IN 625.

The elevated temperature fatigue test results at two strain amplitudes of 0.005 and 0.01 mm/mm, i.e., the reversals to failure, $2N_f$, and the average stress amplitudes at midlife, are presented in Fig. 6 (a)-(c) and (b)-(d), respectively, for the L-PBF/LP-DED IN 625 and L-PBF/LP-DED IN 718. The ranges of fatigue lives ($2N_f$) are presented using bars whose ends indicate the maximum and minimum lives observed for each specimen condition. Fig. 6 (a)-(b) indicated that, in general, both alloys have shown better fatigue performance at 427 °C as compared to those of 649 °C at both strain amplitudes and test temperatures, which could be attributed to the effect of temperature on the strength of both alloys. For IN 625, an increase in temperature in this range can reduce deformation twinning which reduces strength (Kim *et al.*, 2020). For the precipitation hardening IN 718 alloy such as the softening of nickel matrix (N. KAWAGOISHI, 2000).

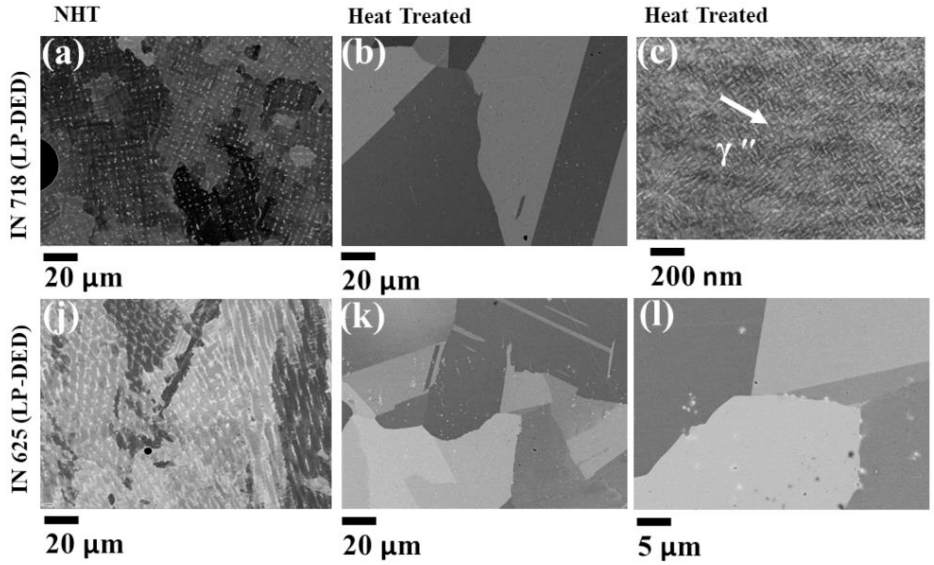

Fig. 4. Typical BSE SEM micrographs obtained in the ND plane (perpendicular to building direction) for some Ni-base superalloys investigated in this study in two heat treated conditions, i.e., NHT and fully heat-treated conditions as listed in Table 3: (a)-(c) LP-DED IN 718 and (d)-(f) LP-DED IN 625.

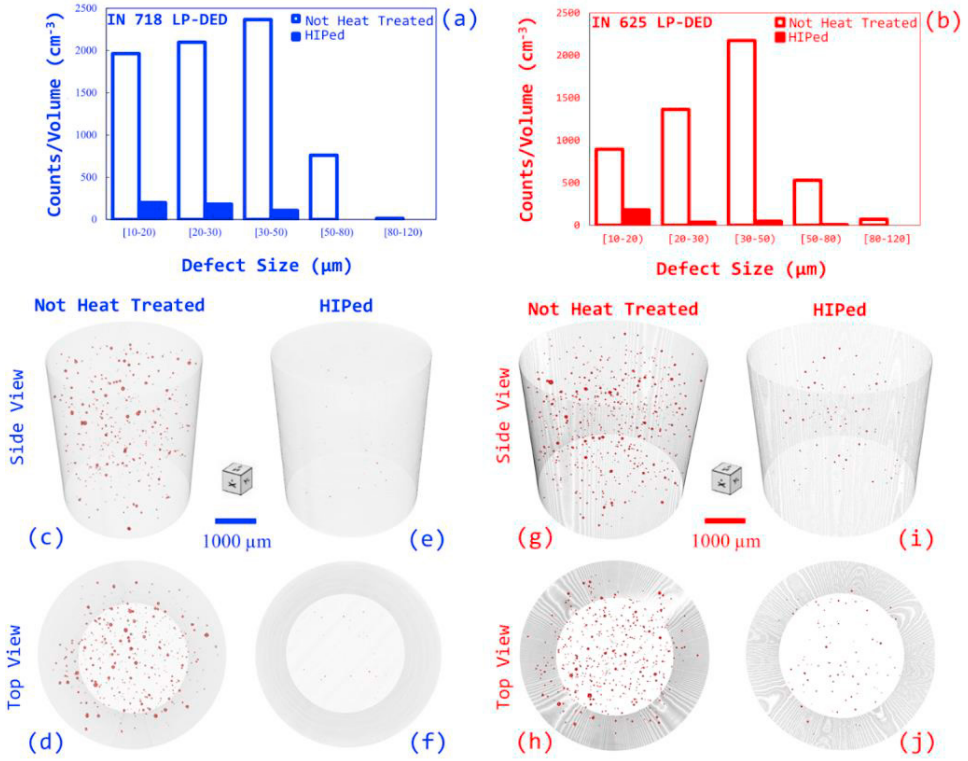

Fig. 5. Typical XCT scan results obtained from the gauge section of IN 718 LP-DED and IN 625 LP-DED test specimens: (a)-(b) defect size distribution measured in average number of defects per unit volume (mm^3); (c)-(d)/(g)-(h) and (e)-(f)/(i)-(j): three-dimensional (side and top) views of the cylindrical scanned volume (ϕ 6.25 mm x 4.27 mm) for NHT and HIPed specimens, respectively, of IN 718 LP-DED/IN 625 LP-DED.

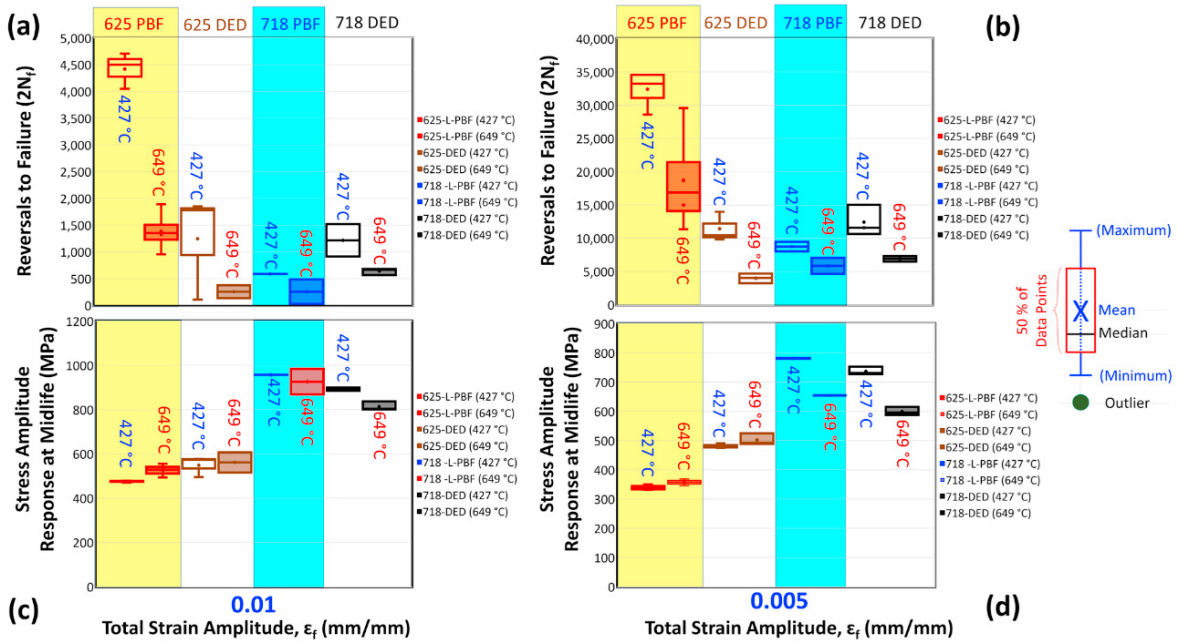

Fig. 6. Fatigue test results for AM IN 625 and IN 718 alloys investigated in this study at two different strain amplitudes, i.e., ε_a = 0.005 and 0.01 mm/mm, and at two elevated temperatures of 424 and 649 °C: fatigue lives in (a)-(b) and stress amplitudes measured for midlife cycle in (c)-(d).

It should also be noted that that the AM IN718 showed inferior fatigue performance at both test temperatures and strain amplitudes in L-PBF condition while in LP-DED condition both alloys offered comparable fatigue performance, which could be attributed to the better ductility in the solid solution IN 625 alloy in general and effect of finer grains observed in L-PBF specimens, respectively. Due to the larger grain sizes for the both the LP-DED IN 625 and IN 718 alloys, the discrepancy in ductility may diminish under elevated temperature. Furthermore, it is shown that the IN 625 has offered better fatigue resistance at both strain amplitudes and test temperatures in L-PBF conditions as compared to the LP-DED ones. However, the inverse is true for the IN 718 alloy, for which, the LP-DED specimens have outperformed the L-PBF ones at both strain amplitudes and test temperatures. This improving effect of larger grain size on fatigue performance of IN 718 at high temperature has been reported in the literature before (KOBAYASHI *et al.*, 2008).

Furthermore, Fig. 6 (c)-(d) shows that IN 718 in both L-PBF and LP-DED conditions at all strain amplitudes and test temperatures have a significantly higher stress levels at midlife as compared with those of IN 625, which could imply that the former has a higher load bearing capability. This could possibly be ascribed to higher strengths in the IN 718 alloys due to the precipitation hardening effect of strengthening ɤ”-phase (Nezhadfar, Johnson and Shamsaei, 2020).

4. Summary and Conclusions

In this study, the fatigue behavior of L-PBF/LP-DED IN 625 and L-PBF/LP-DED IN 718 alloys were studied and compared at two strain amplitudes of 0.005 and 0.01 mm/mm and at two elevated temperatures of 427 and 649 °C. The test specimens were fully heat-treated using a multiple-step procedure including stress relief at 1066 °C for 1.5 hr, followed by HIP at 1065 °C for 3.5 hr under 100 MPa plus solution treatment at 1177 °C for 1 hr for IN 718 and at 1135 °C for IN 625 and plus standard 2-step ageing processes for IN 718. A summary of the experimental observations made in this study is listed below:

- The BSE micrographs reveal that the grain structure of the test specimens was homogenized upon heat

treatment and the prior inter-dendritic regions are dissolved for LP-DED specimens. Furthermore, it was observed that that the microstructure of the LP-DED specimens possess slightly larger grain sizes than those of the L-PBF counterparts, which could be attributed to the higher cooling rate experienced during the L-PBF process as well as higher layer height used in fabrication process of the LP-DED specimens.

- The fatigue test results revealed that both IN 625 and IN 718 alloys have shown better fatigue performance at 427 °C as compared to those of 649 °C at both strain amplitudes investigated, which could possibly be attributed to the effect of temperature on deformation mechanisms. For IN 625, higher temperature reduces twinning, resulting in reduced strength and for IN 718, higher temperature result in softening of nickel matrix.
- The AM IN718 showed inferior fatigue performance at both strain amplitudes and test temperatures in L-PBF condition, while in LP-DED condition both alloys offered relatively comparable fatigue performance. This could be attributed to the better ductility in the solid solution IN 625 alloy in general and the effect of finer grain sizes observed in L-PBF specimens, respectively.
- Furthermore, it was observed that IN 625 has offered better fatigue properties at both strain amplitudes and test temperatures in L-PBF conditions as compared with those of LP-DED ones whereas the IN 718 alloy offered a better fatigue behavior in LP-DED conditions. This could possibly be attributed to improving effect of larger grain size on fatigue performance of the precipitation hardening IN 718 at high temperatures.

Acknowledgements

This material is based upon the work partially supported by the National Aeronautics and Space Administration (NASA) under Cooperative Agreement No. 80MSFC19C0010. This material is also based upon work partially supported by the National Science Foundation (NSF) under grant No. 1919818.This paper describes objective technical results and analysis. Any subjective views or opinions that might be expressed in the paper do not necessarily represent the views of the National Aeronautics and Space Administration (NASA) or the United States Government.

References

Antolovich, S. D. and Armstrong, R. W. (2014) 'Plastic strain localization in metals: origins and consequences', *Progress in Materials Science*, 59, pp. 1–160. doi: 10.1016/j.pmatsci.2013.06.001.

Antolovich, S. D., Rosa, E. and Pineau, A. (1981) 'Low cycle fatigue of René 77 at elevated temperatures', *Materials Science and Engineering*, 47(1), pp. 47–57. doi: 10.1016/0025-5416(81)90040-9.

ASTM International (2012) 'ASTM E3-11: Standard Guide for Preparation of Metallographic Specimens'. doi: 10.1520/E0003-11R17.1.

ASTM International (2014a) 'ASTM F3055-14a Standard Specification for Additive Manufacturing Nickel Alloy (UNS N07718) with Powder Bed Fusion'. doi: 10.1520/F3055-14A.

ASTM International (2014b) 'ASTM F3056-14a: Standard Specification for Additive Manufacturing Nickel Alloy (UNS N06625) with Powder Bed Fusion'. doi: 10.1520/F3056-14E01.

ASTM International (2019) 'E606/E606M - 19e1: Standard Test Method for Strain-Controlled Fatigue Testing'. doi: 10.1520/E0606_E0606M-19E01.

Donachie, M. J. and Donachie, S. J. (2002) *Superalloys: A Technical Guide*. 2nd edn, *America*. 2nd edn. Materials Park, OH: ASM International. doi: 10.1361.

Ghiaasiaan, R. *et al.* (2021) 'Superior tensile properties of Hastelloy X enabled by additive manufacturing', *Materials Research Letters*. Taylor and Francis Ltd., 9(7), pp. 308–314. doi: 10.1080/21663831.2021.1911870.

Kim, K.-S. *et al.* (2020) 'High-temperature tensile and high cycle fatigue properties of inconel 625 alloy manufactured by laser powder bed fusion', *Additive Manufacturing*, 35, p. 101377. doi: 10.1016/j.addma.2020.101377.

KOBAYASHI, K. *et al.* (2008) 'High-temperature fatigue properties of austenitic superalloys 718, A286 and 304L', *International Journal of Fatigue*, 30(10–11), pp. 1978–1984. doi: 10.1016/j.ijfatigue.2008.01.004.

N. KAWAGOISHI, Q. C. and H. N. (2000) 'Fatigue strength of Inconel 718 at elevated temperatures', *Fatigue Fract Engng Mater Struct*, 23, pp. 209–216.

Nezhadfar, P. D., Johnson, A. S. and Shamsaei, N. (2020) 'Fatigue behavior and microstructural evolution of additively manufactured Inconel 718 under cyclic loading at elevated temperature', *International Journal of Fatigue*, 136, p. 105598. doi: 10.1016/j.ijfatigue.2020.105598.

Shao, S. *et al.* (2017) 'Solubility of argon in laser additive manufactured α-titanium under hot isostatic pressing condition', *Computational Materials Science*, 131, pp. 209–219. doi: 10.1016/j.commatsci.2017.01.040.

Zaefferer, S. and Elhami, N.-N. (2014) 'Theory and application of electron channelling contrast imaging under controlled diffraction conditions', *Acta Materialia*, 75, pp. 20–50. doi: 10.1016/j.actamat.2014.04.018.